IJISET - International Journal of Innovative Science, Engineering & Technology, Vol. 6 Issue 1, January 2019
ISSN (Online) 2348 – 7968
www.ijiset.com

Fractures and Vuggy Pores, as Deduced from Formation Micro Imager log and Petrophysical Data of the Miocene Syn-rift Dolomite Reservoir, Issaran Field, Western Shore of the Gulf of Suez, Egypt.

Ali Younis[1], Othman, A.A.[2], Mohamed Abd El-Aal[3], Emad A., Abd El Aziz[1*]

[1]Geophysical Sciences Department, National Research Centre, Cairo, Egypt.
[2]Department of Geology, Faculty of Science, Al-Azhar University, Cairo, Egypt.
[3]Department of Geology, Faculty of Education, Ain shams University, Cairo, Egypt.
[*] Corresponding author (e-mail: emadnrc2002@yahoo.com)

Abstract

Fractures and the connected vuggy pore spaces within a reservoir play an influential role in the porosity and permeability, therefore affect the fluid flow. The present study is concerned with the identification of fractures and vuggy pores for the lower dolomite reservoir in the field area, in addition to the role of lithology on the fracture parameters. Computer-assisted log analyses were used to evaluate the petrophysical parameters, such as shale volume, secondary porosity, effective porosity, water saturation, hydrocarbon saturation, flushed-zone saturation and reservoir and pay flags. Cross-plots of the petrophysical parameters versus depth were illustrated. Moreover, the cross-plots were used to show the lithologic and mineralogic components. The formation borehole imaging tool (FMI) and conventional well log data have been used to study the secondary porosity of the studied rock unit. The obtained data revealed that, the lower dolomite reservoir is intermittently vuggy with solution filled channels. The vuggy pores are observed to be well connected, which supports good effective porosity values interpreted from petrophysical data. The abundance of secondary porosity (Fractures and vugs) in the lower dolomite reservoir would play a key role in evaluating its reservoir quality and reservoir performance.

Key words: Petrophysical characteristics, fractures and vugs, dolomite reservoir, Issaran Field, Egypt.

Introduction

Many productive carbonates have complex dual porosity systems with widely varying proportions of primary and secondary porosity. The secondary porosity may contain vugs, moulds, channels, and fractures. Moreover, the originally homogeneous matrix / intergranular primary porosity may become patchy through selective cementation of the matrix. On the conventional porosity logs (density, neutron, and sonic), these porosity types often appear somewhat uniformly distributed. Moreover, due to coarse resolution of the conventional tools, such types of porosity get underestimated or overlooked (Movahed, 2007). Borehole electrical images, FMI (Formation Micro Imager) in particular, provide both high resolution and azimuthal borehole coverage to resolve quantitatively the heterogeneous nature of porosity components.

The study area is in the Issaran Field, which lies in the NW onshore part of the Gulf of Suez rift. The field is located 290 km southeast of Cairo and 3 km inland from the western shore of the central province of the Gulf of Suez covering an area of 20000 acres (Fig. 1). It lies in the central dip province of the rift where pre-rift and syn-rift rocks dip towards the NE (Moustafa, 1976 and Patton et al., 1994).

The present study is an attempt to indicate the role of fracture and vugs on the reservoir parameters for the Miocene syn-rift fractured lower dolomite reservoir in one of the world class rift basins. For this aim petrophysical and image logs are utilized to produce an integrated study of secondary porosity evaluation of the studied reservoir.

General Geology

The stratigraphic sequence encountered in the Issaran Field is ranging in age from Pliocene-Recent to Paleozoic. In the study area, the Miocene section includes five rock

units, namely from base to top: Nukhul dolomite, Gharandal carbonates, lower dolomite, upper dolomite and Zeit sand, which similar to a marginal facies as those observed in the deep parts of the Gulf of Suez (Fig. 2).

The pressure on all zones is very low and considered being below the normal gradient. According to Samir (2010), out of the five rock units, three of them have been produced by applying cyclic steam injection. The first, is the Zeit Sand, rock unit which has a 12 ft as a pay zone. The second, is the upper dolomite unit, which is characterized by a depleted fractured dolomite reservoir and has an average thickness of 400 ft, with the top of the formation located at 1,000 ft and has an average pressure of 250 psi. The third, is the lower dolomite rock unit, which located at 1,500 ft and has almost close characteristics and an average thickness as the upper dolomite reservoir. Both the upper and lower dolomite rock units have been produced through applying the cyclic steam injection technology. The field cumulative production has been increased after applying the new technologies and the right reservoir management practices from 1.5 MMSTB (the oil produced from the field was discovered and before applying these techniques) to more than 10 MMSTB during the last 10 years. Moreover, for the upper and lower dolomite rock units, the steam injection project considers the first successful cyclic steam project in the Middle East (Zuhair et al., 2014).

Dolomite reservoir is subdivided into upper dolomite and lower dolomite with by the intra dolomite shale in between. The upper dolomite almost entirely composed of dolomite with few thin beds of shale. Nodular anhydrite is occurring disseminated in dolomite oras interbedd lamina. Porosity is commonly oil saturated; vuggy porosity to pinpoint porosity. Sub-vertical fractures, both open and filled with anhydrite were noted in Issaran well-1.

The intra dolomite shale is black to green dolomitic shale about 20 ft thick with some interbedded dolomite. It separates the upper and lower dolomite reservoirs and

provides a cap rock for the oil accumulations in the lower dolomite reservoir (E.G.P.C., 1996).

The lower dolomite rock unit is considered to be the main target of the present study. The Isopach map of the lower dolomite rock unit (Fig. 3) reflects that, the thickness gradually increasing towards southeastern part in the study area. The maximum thickness penetrated of the lower dolomite rock unit is 561 ft in CSS-307 well. The minimum thickness cannot be precisely determined since the wells with minimum thickness are faulted out.

The structural contour depth map on top of the lower dolomite unit (done using Petrel 2009 software) and the 3-D interpreted structural seismic section (Figs. 4 & 5) reveals that, the study area is a NE-tilted fault block bounded by NW-SE oriented (clysmic trend) and N-S to NNE-SSW oriented (Aqaba trend) normal faults, forming trap door structures. The faults (F1 and F3) form a graben system structure taking the direction of NW-SE. Such a high structure exists in the middle parts along the up throw blocks of the major fault affecting in the study area. The average vertical fault throws are ranged from 60 to 520 ft, while they make horizontal displacements for the beds ranged from 25 to 340 ft.

Materials and Methods

The borehole data of study wells in Issaran Field, including the different types of open-hole logging suits are used in this study. Among these wells, two wells (CSS-303 and CSS-329) have an available FMI image log.

Open-hole log data; such as resistivity logs, neutron, density, sonic and gamma-ray for the studied rock unit were collected and digitized. This study has been carried out through qualitative and quantitative analyses by means of the Interactive Petrophysic (IP) software. Cross-plots were used to show the lithologic and mineralogic components of the lower dolomite reservoir. The shale content was calculated from gamma-ray, neutron, neutron-density and resistivity logs. The minimum shale content

given by these shale indicators is likely to be close to the actual value of the shale content. The corrected porosity was determined using a combination of the density and neutron logs, after applying various environmental corrections. The water saturation was computed with the Indonesian equation. Corrected well logs and reservoir parameters, which are derived from them, are plotted versus depth, through the vertical cross-plots and lithology identification cross-plots. These cross-plots give a quick view about the rock and mineral contents in a qualitative way. Some of these cross-plots give the amounts of lithologic contents in a quantitative way. Such cross-plots are the neutron-bulk density and M-N cross-plots. Sonic versus neutron-density cross-plot has also been produced to classify the type of porosity between primary and secondary. Sonic porosity is calculated based on the Wyllie Equation.

The response of various types of resistivity measurements can be utilized to indicate fractures. In reservoirs with very low porosity, the dual laterolog can greatly be affected by the presence of fractures, especially those filled with conductive mud. So, vertical, subvertical and horizontal-filled fractures can be detected by the relative increase of conductivity, which they provide. Due to its short depth of investigation, shallow laterolog log (R_{LLs}) is much affected than the deep laterolog log (R_{LLd}) and a comparison of these resistivities in front of fractured zones will result in resistivity ratio less than one as the shallow laterolog resistivity will be less than the deep one (Abd El-Rahman and Lashin, 2004). Furthermore, the interpretation of the FMI data is done to characterize geological features around the drilled borehole, such as fractures, bedding planes and voids/vugs or channels. The conventional logging data were combined with the FMI image log of some wells, applying the qualitative response of the different logging tools.

Results and Discussions

Lithology:

The Lithology can be one of important factor in controlling fracture distribution. Dolomite reservoirs are important sources of hydrocarbons, and their fluid flow pattern is commonly influenced by fractures. Fracture architecture depends on the rock properties at the time of fracturing (particularly subcritical crack index). Lithology and bed thickness are primary controls the fracture density, fracture aperture and orientation, reflecting the fact that different rock unit is mechanically distinct. Fracture density has been correlated with the mineralogical composition of the matrix grain, porosity and bed thickness. More brittle rocks will have more density fracture rather less brittle rocks. The primary brittle constituent within a rock are quartz, dolomite and calcite.

The analysis of the available well logging data (Figs. 6 & 7) demonstrates the typical dolomite behavior of this reservoir. Figure (6) shows the density-neutron cross-plots of the study area, where as the majority of data points are clustered along the dolomite lithology line. The M-N plot (Fig. 7) assigns the same dolomitic lithology, with data points shifted toward the secondary porosity direction. Some data points are occupied in the area between the dolomite and the approximate shale part, indicating the presence of anhydrite. In the present study, dominated mineral is dolomite and anhydrite, calcite and shale are little.

Well-logs data analysis:

Figures (8 & 9) exhibit the petrophysical log data and Formation Micro Imager (FMI) of two selected wells in Issaran Field (CSS-303 and CSS-329). The display of these figures is given for the lower dolomite rock unit. These wells are selected to demonstrate the characteristics of the changes in the lithological composition, water and hydrocarbon saturation with effective porosity, in addition to some well log data as spectral gamma ray and caliper. FMI image logs viewed in static and dynamic views

while fitting sine waves to observed bed boundaries, fractures, and other geologic features. Static images have one contrast setting for the entire well, providing a view of relative changes in rock resistivity throughout the borehole. Dynamic images have variable contrast applied in a moving window, providing enhanced views of features including vugs, fractures, and bed boundaries. Dynamic images reflect detailed features in rocks that have very low resistivity; e.g. shales, and very high resistivity; e.g. carbonates and crystalline rocks. Fractures in the subsurface analysis were characterized as either natural or induced features. They were also classified as conductive or resistive features, representing possibly open; water-filled or closed; mineralized fractures, respectively. The azimuths and dips of interpreting geologic features are presented in a tadpole plot. The vertical scale is depth and the horizontal scale is dip (0°-90°).

From the obtained results, it is observed that the general lithology from composite log is strongly confirmed by the interpretation from calculations. The lithology of the lower dolomite reservoir is uniform and mainly dolomitic in composition. The studied rock unit in the two wells are intercalated with shale content which varies from 5 % in CSS-329 well to 9 % in CSS-303 well as average values. The pore spaces are uniform all over the whole section, except in the lower part of the interval in CSS-329 well. This well includes a high resistivity oil bearing interval at the top and a low resistivity non-pay interval at the base. This zone is a highly fractured zone and related to a certain mechanical layer within the lower dolomite reservoir. This mechanical layer is indicated on the conventional well-logs as a layer of higher density and lower porosity readings from density-neutron logs and lower sonic log readings than the overlying and underlying rocks; that is, it is a tight zone that corresponds to a brittle layer within the lower dolomite reservoir (Saoudi et.al., 2014).

Both secondary porosity and effective porosities, derived from the wire-line log data, are characterized by high fluid (water and hydrocarbon) saturations. The zones

with the highest secondary porosity are labeled (A - H) and (1 - 6) are the intervals where image logs utilized. Secondary porosity for the CSS-329 well is higher compared to CSS-303 with the zones of the highest level of the secondary porosity located in oil bearing intervals. High fracture density occurs primarily in dolomites with low porosity and high density. The estimated hydrocarbon saturation is about 80 % in CSS-329 well and is concentrated mainly in the upper part of the section (Fig. 8) to 83 % in CSS-303 well distributed all over the section (Fig. 9). Based on the lithological, petrophysical and fluid analyses, the studied interval has been differentiated into the reservoir and pay flags.

The (neutron-density) porosity and (sonic) porosity cross-plot (Fig. 10) is used for the determination of the type of porosity (primary or secondary) in the evaluated zones (Steiber, 1973). This cross-plot indicates the dominance of the high secondary porosity with low primary (inter-granular) porosity type.

The resistivity-ratio cross-plot (Fig.11), showing the effect of fractures on the laterolog measurements. Analysis of cross-plot revealed that, the fractured shale, clean, massively fractured and hydrocarbon zones, respectively. All the data points are located along the unit ratio resistivity line (R_{LLd} / R_{LLs} =1) in the area characterized by its non-fracture nature. Water-filled fracture porosity will have a ratio of R_{LLd} /R_{LLs} greater than one, with R_{LLd} reading less than that expected for an equivalent amount of intergranular porosity. For hydrocarbon-bearing fractures, the ratio also will be greater than one, but the RLLd value will be higher than that seen in water-filled fracture porosity. Water-bearing fractured zones plot along line A, while points plotting to the northeast of this line represent zones of significant fracture porosity containing hydrocarbons.

Good identified fractured zones are indicated in the upper dolomite rock unit, where the majority of data points are clustered in the water bearing fracture area with the increasing order of the R_{LLd} values in ISS-100 and CSS-329 wells and above the

resistivity ratio line of value 2 (R_{LLd} / R_{LLs} > 2) along a trend of increasing of resistivity from the water bearing fracture area to the massively hydrocarbon and hydrocarbon bearing fractured areas. This is supported by the good and wide resistivity separations between the shallow and deep laterologs, especially in CSS-303 well.

Evaluation of secondary porosity from Formation Micro Imager (FMI):

The hard rocks, especially dolomite, are susceptible to dissolution and fracturing (secondary porosity). The pore types could be a matrix, fractures and vugs or a combination of these. The variation in fracture density with matrix porosity, lithology, texture and pore-pace type links to the mechanical properties of the rocks. The diagenetic steps, especially the dolomitization, affected the mechanical properties of some of the layers in the upper and lower dolomite reservoirs, which in turn affected the fracture formation (Ameen et.al., 2010).

Figures (12 & 13) show that, the evaluated lower dolomite rock unit is considerably affected by the diagenesis, which resulted in the creation of several types of secondary porosity structures. The major secondary porosity features identified in studying wells are vugs, drilling-induced factures and channels.

Vugs:

Vugs are pore spaces in rocks that are typically formed by any of the cracks and fissures opened by tectonic activity, open spaces within ancient collapse breccias, dissolution or erosion of mineral crystals or fossils inside a rock matrix. Vuggy porosity is divided according to how the pore space is connected into separate vugs (such as ooids or skeletal material, and intrafossil porosity) and touching vugs. The isolation of separate vugs adversely affects the permeability (Shalaby et.al., 2018).

FMI indicates that vuggy pores are very abundant and dominant across the whole studied interval (indicated by blue arrows). These vugs vary in size and exist in forms of isolated and interconnected vugs. A majority of large isolated vugs is located in the interval of 1550-1580 ft., and at 1950 - 1980 ft., in CSS-329 well (Fig. 12a & b). A

large interconnected vugs network exists in intervals of 1583-1464 ft., in CSS-329 well (Fig. 12a), and 1640-1750 in CSS-303 well (Fig. 13a). The interconnected vugs of various sizes observed at 1650-1770 ft., and. 1930-1950 ft in CSS-329 well (Fig. 12b&c). The poorly interconnected vugs pores at interval between 1751-1890 ft in CSS-303 well (Fig. 13b).

Fractures:

The image logs identified fractures include open and closed fractures, which have the same attitudes. The identification of closed fractures on image logs is by virtue of their high resistivity. Resistive fractures on image logs are conventionally known to correspond to cemented fractures (Ozkaya and Minton 2007).

Drilling-induced fractures are a product of drilling and depends on the rock properties. When the drilling pressure exceeds the elasticity limit of the rock, it may not be able to withstand this pressure and may fracture as a result. Carbonates are relatively highly rigid in nature, and consequently have low elasticity, which makes them more susceptible to fracture. Unlike natural fractures that tend to cross-cut the wellbore, Drilling-induced fractures typically develop as narrow, sharply defined features that are sub-parallel or slightly inclined to the borehole axis in vertical wells.

Drilling-induced vertical fractures interconnected to natural fractures channel (indicated by gray and green arrows respectively) can be seen in CSS-329 well at the interval between 1770 ft and 1930 ft (Fig. 12b) and are almost parallel to the borehole. Whereas, in CSS-303 well can be seen in the interval between 1751 ft and 1850 ft (Fig. 13b).

Channels:

The lower dolomite rock unit in the CSS-329 and CSS-303 wells has numerous dissolution channels indicated by the pink arrows (Figs. 12b and 13b). Generally, from the borehole image logs, the studied rock unit contains abundant secondary porosity structures, including vugs, fractures and channels. Location of the zones with these

structures correlates with the depths of the zones having higher secondary porosity values according to the interpretation of the well logging data.

Conclusions

Petrophysical characteristics derived from conventional well log data indicate that, the highly fractured zone of the lower dolomite reservoir probably corresponds to a mechanically brittle layer within the dolomite section. In addition to the natural fractures affecting this brittle layer, drilling-induced fractures exist in a relatively large number, as seen in the image logs of wells. This brittle layer was fractured during drilling under the effect of the present-day stress field, leading to the development of additional fractures in this zone. The lower dolomite rock unit contains abundant secondary porosity structures, including vugs, channels and fractures. Location of the zones with these structures correlates with the depths of the zones having higher secondary porosity values according to the interpretation of the well logging data.

Secondary pores are located in hydrocarbon reach zones with hydrocarbon saturation levels of over 80%. Application of the formation borehole imaging tools enabled further understanding of the types and morphological configuration of these secondary pore spaces, which could not be identified by the well logging data. FMI images confirm the presence of different secondary porosity structures, which are vugs, drilling-induced fractures and dissolution channels, across the evaluated depth intervals. The vugs are observed to be interconnected, which support the evaluation of the petrophysical data for the same well, which reveals that the average effective porosity is 16% across the pay studied interval.

References

Abd El-Rahman, A. Y. A. and Lashin, A., 2004. Evaluation of the Basement reservoir rocks in some selected wells in North Gulf of Suez and South Sinai, Egypt. Annals Geol. Surv. Egypt, V. XXVII, pp. 459-477.

Ameen, M. S., Buhidma, I. M. and Rahim, Z., 2010. The function of fractures and in-situ stresses in the Khuff reservoir performance, onshore fields, Saudi Arabia, AAPG Bull., V. 94, pp. 27-60.

Egyptian General Petroleum Corporation, 1996. Gulf of Suez oil and gas fields, A comprehensive overview. Cairo, Egypt, pp. 520-528.

Moustafa A. A. E., 1976. Block Faulting in the Gulf of Suez. 5th Exploration Seminar, Cairo, Egypt, pp. 1-19.

Movahed, Z., 2007. Enhanced reservoir description in carbonate and castic reservoirs, Paper presented at the SPE Asia Pacific oil & Gas Conference and Exhibition, Jakarta, Indonesia, 30 Oct. - 1 Nov. http://wwwtmupn. blogspot.com/2007/10/spe-asia-pasificoil-gas-conference.

Ozkaya,S. I. and Minton, K. R., 2007. Flow potential of fracture corridors and large conductive fractures in a clastic reservoir, Oman. In: Lonergan, L., Jolly, R. J. H., Rawnsley, K. and Sanderson, D. J. (Eds) Fractured reservoirs. Geological Society, London, Special Publications, 270, pp. 245-263.

Patton, T. L., Moustafa, A. R., Nelson, R. A. and Abdine, A. S., 1994. Tectonic evolution and structural setting of the Gulf of Suez rift. In: Landon, S. M. (Ed.) Interior Rift Basins. AAPG, Memoirs, 59, pp. 9–55.

Samir, M., 2010. Rejuvenation Issaran Field - Case study. SPE 127847, 14 pp.

Saoudi, A., Moustafa, A. R., Farag, R. I., Omara, M. M., Wally, H., Fouad, A., Tag, A., and Ragab, R. Z., 2012. Dual-porosity fractured Miocene syn-rift dolomite reservoir in the Issaran Field (Gulf of Suez, Egypt): a case history of the zonal isolation of highly fractured water carrier bed Geological Society, London, Special Publications, 374, first published on September 5, 2012, doi: 10.1144/SP374.7

Shalaby, M. R., Jumat, N. and Islam, M. A., 2018. Formation Microscanner providing better answers for carbonate secondary porosity in Alamein dolomite Formation, NW Desert, Egypt. Geosciences, 16 P.

Steiber, R.G., 1973. Optimization of shale volumes in open hole logs. J. Pet. Tech., 31: pp. 147-162.

Zuhair, A., Hussain, A., and Mohammed, A., 2014. An overview of steam injection projects in fractured carbonate reservoirs in the Middle East. Journal of Petroleum

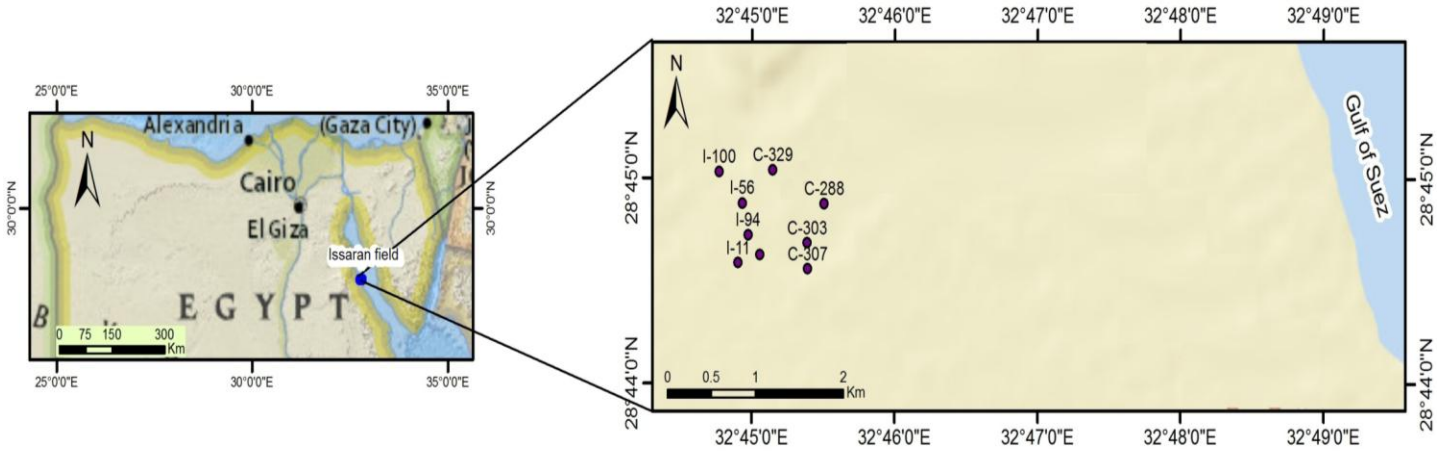

Figure 1: Location map of the studied wells, Issaran Field, Western shore of the Gulf of Suez, Egypt.

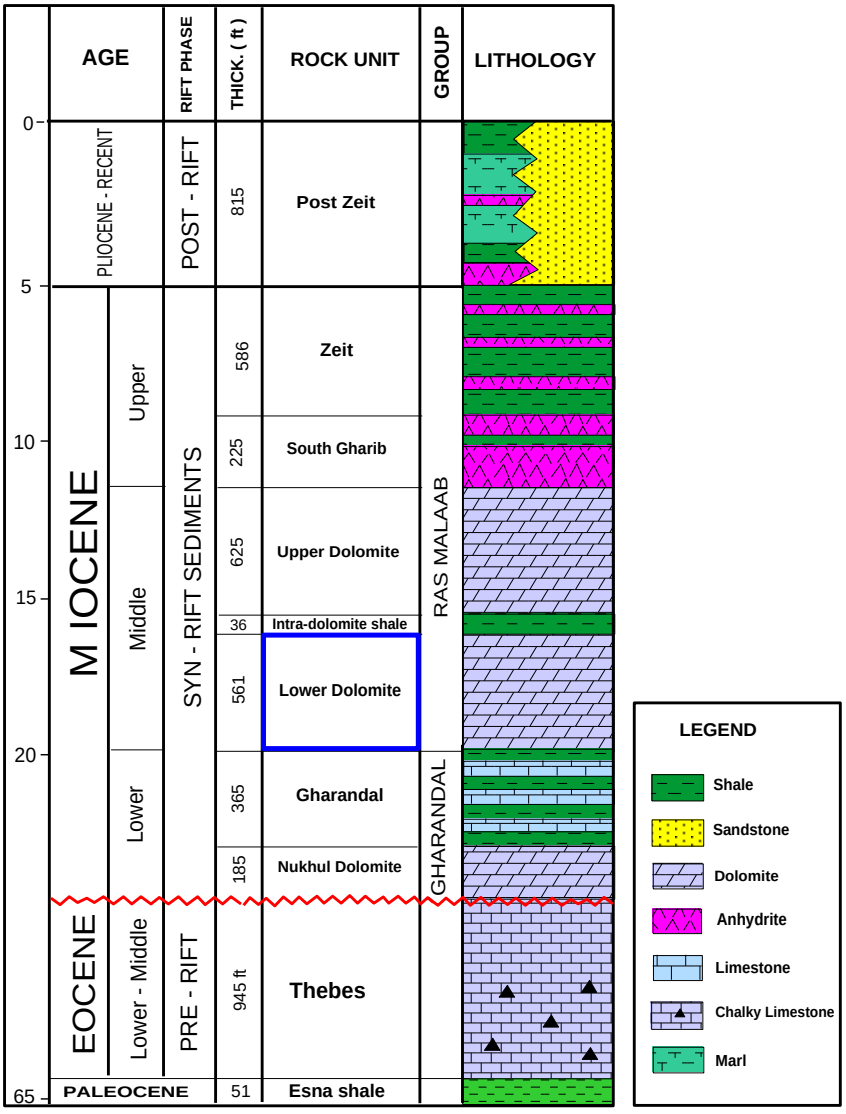

Figure 2: Stratigraphic column showing the detailed portion of the Miocene rocks represents in Issaran Field.

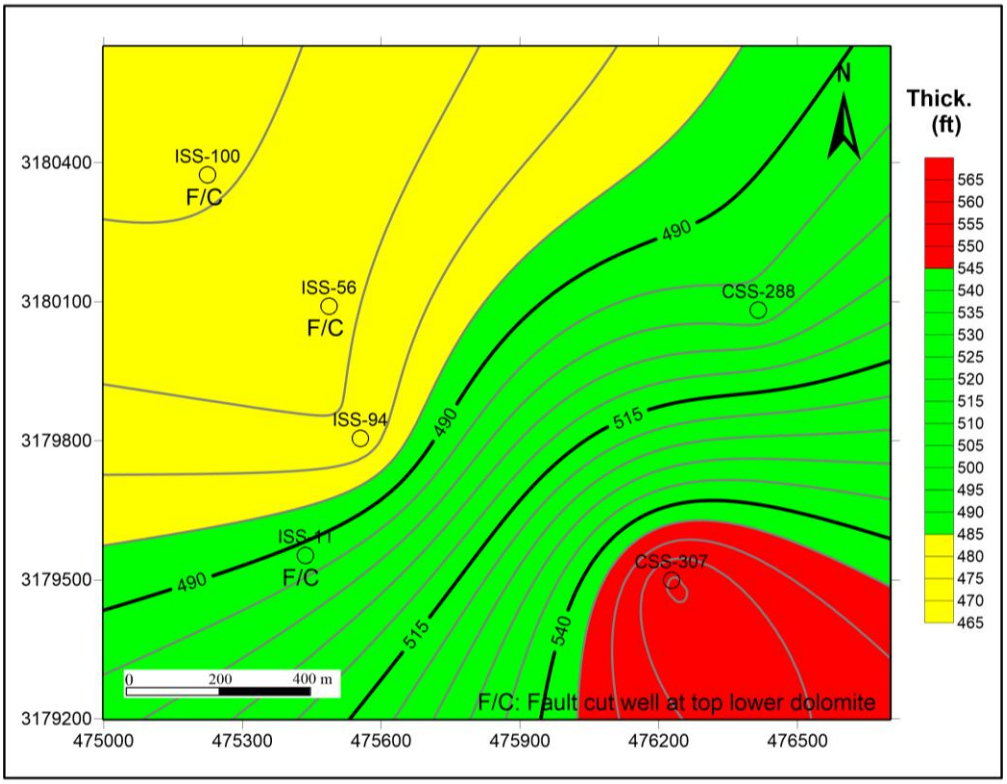

Figure 3: Isopach map of the lower dolomite rock unit in the study area, (C.I = 5 ft.).

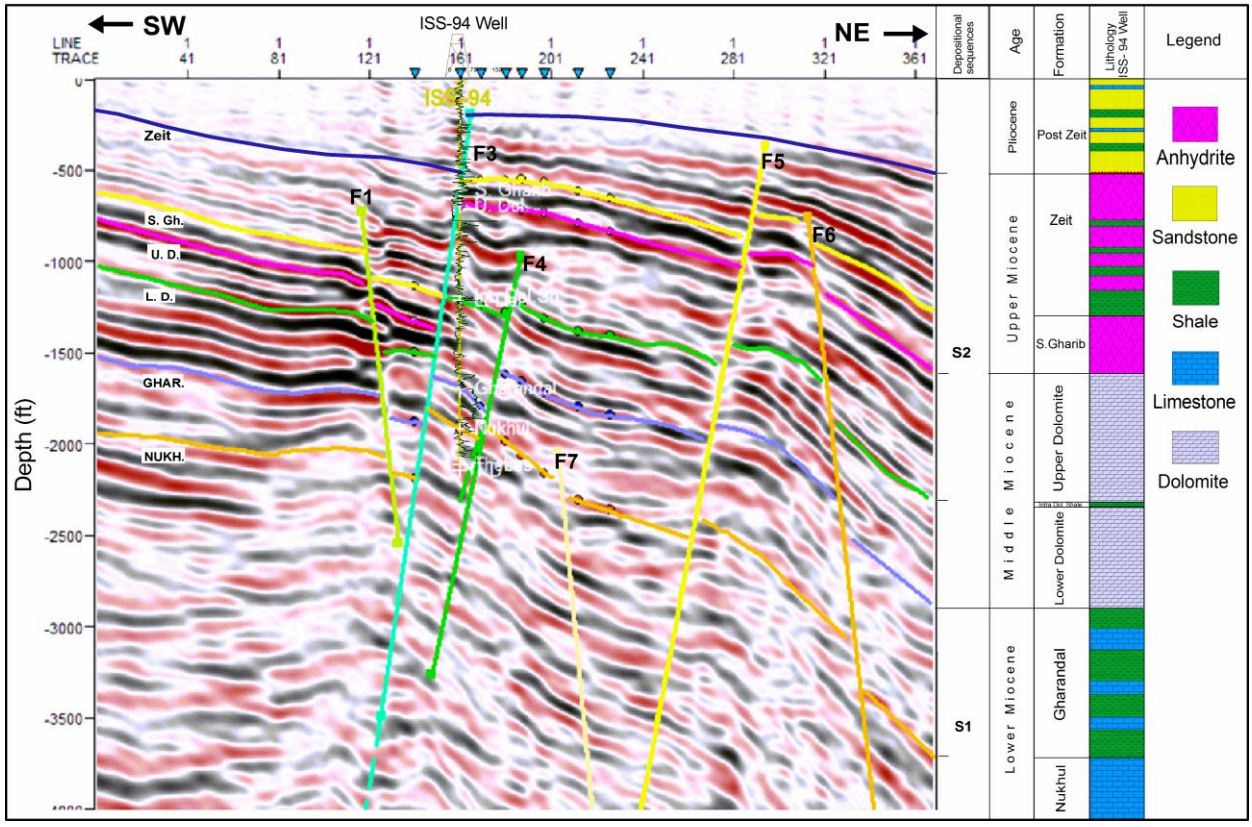

Figure 4: Interpreted seismic reflection profile (L11985) showing the identified structural elements.

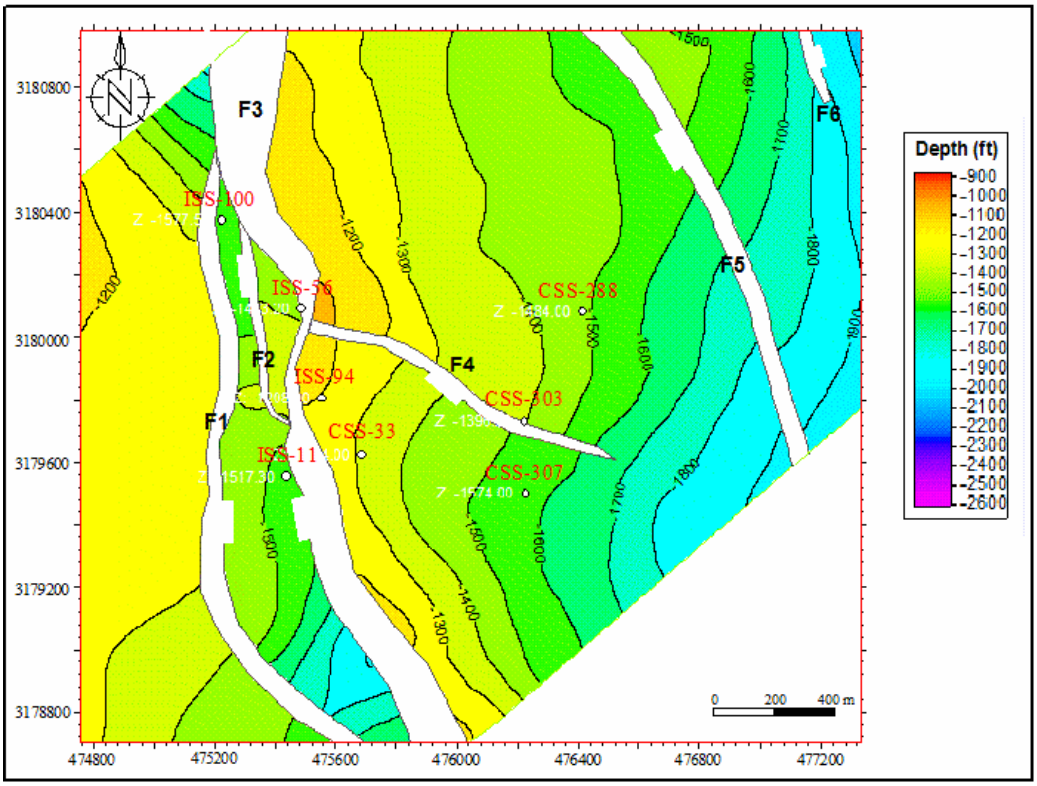

Figure 5: Structure contour depth map on top lower dolomite rock unit in the study area, (C.I. = 100 ft.).

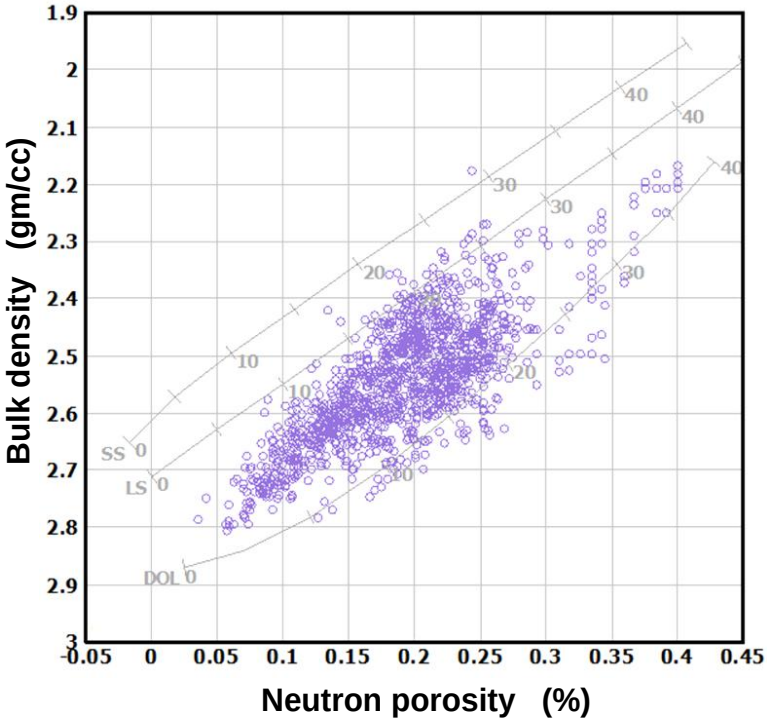

Figure 6: Neutron porosity and bulk density cross-plot of the lower dolomite rock unit in the study area.

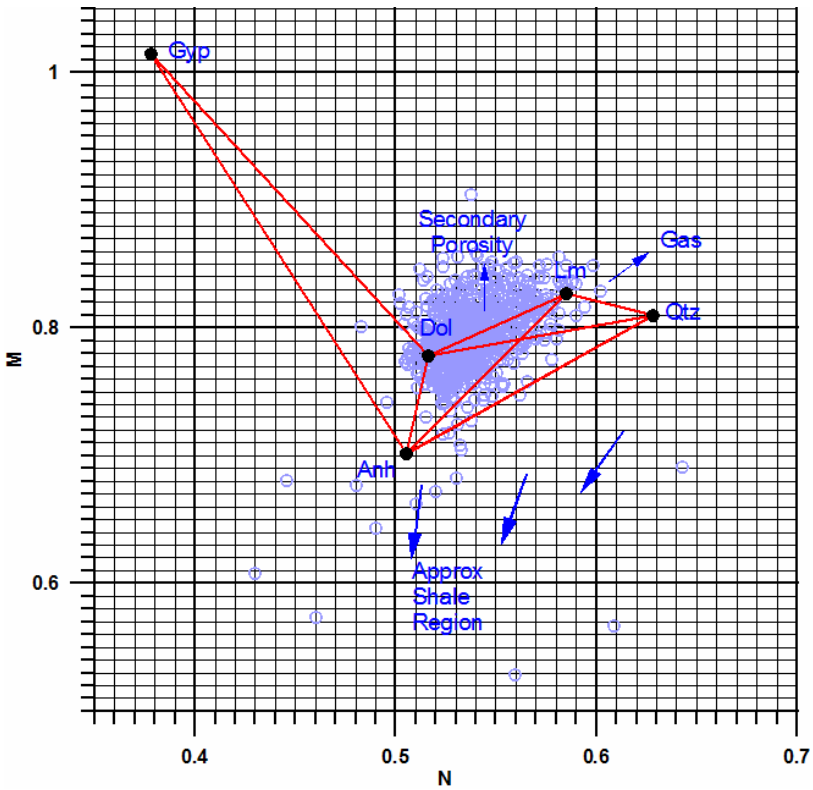

Figure 7: M-N plot showing lithological components of the lower dolomite rock unit in the study area.

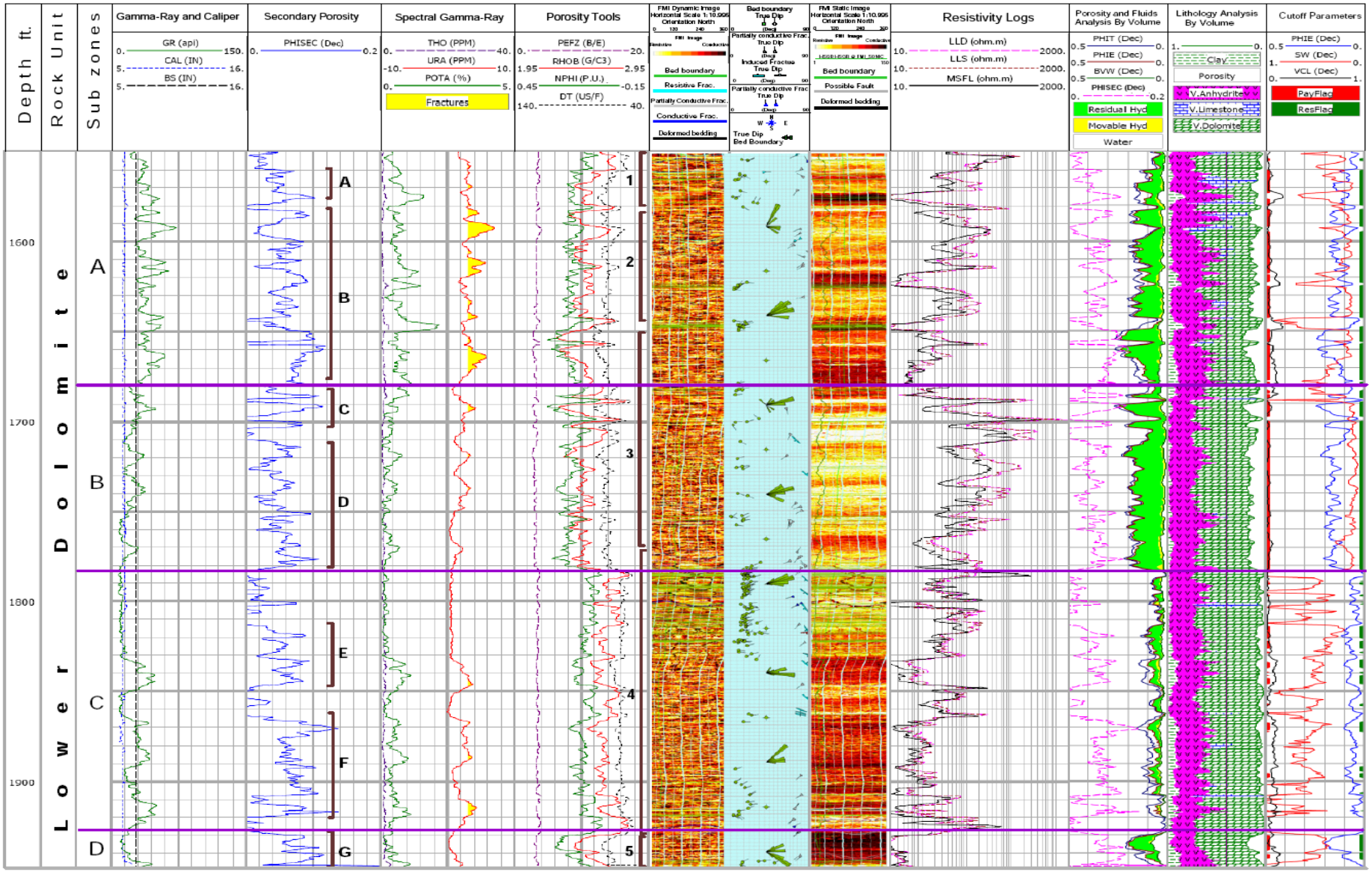

Figure 8: Combination between the petrophysical characteristics derived from conventional well log data and FMI (Formation Micro Imager) showing high secondary porosity in the lower dolomite reservoir, CSS-329 well, where the zones with greatest secondary porosity are labeled (A-G) and (1- 6) are intervals where image log is utilized.

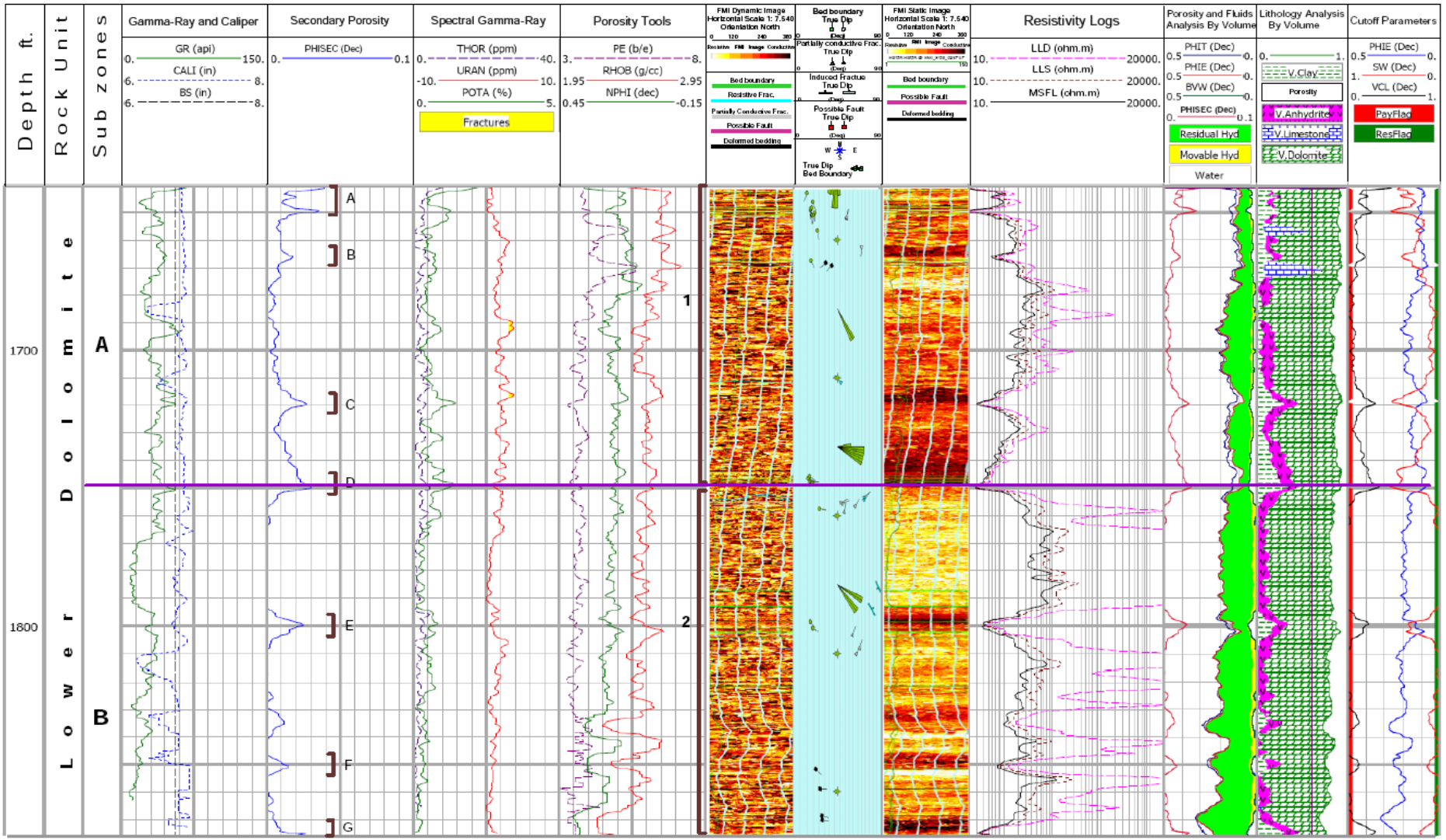

Figure 9: Combination between the petrophysical characteristics derived from conventional well log data and FMI (Formation Micro Imager) showing high secondary porosity in the lower dolomite reservoir, CSS-303 well, where the zones with greatest secondary porosity are labeled (A-H) and (1&2) are intervals where image log is utilized.

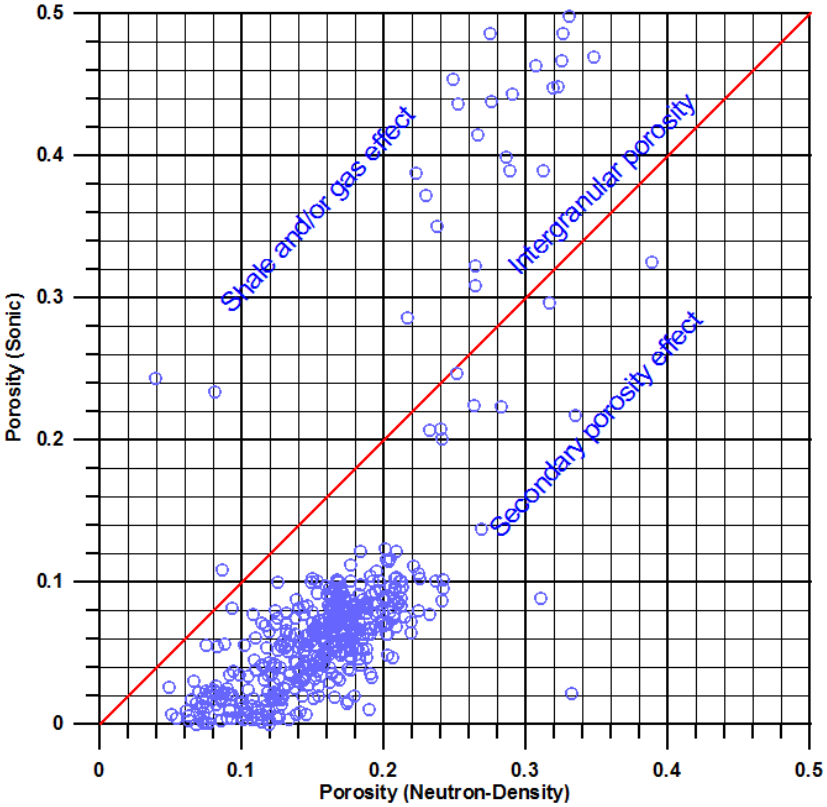

Figure 10: Cross-plot of porosity (neutron-density) versus porosity (sonic) showing type of porosity of the lower dolomite reservoir in the study area.

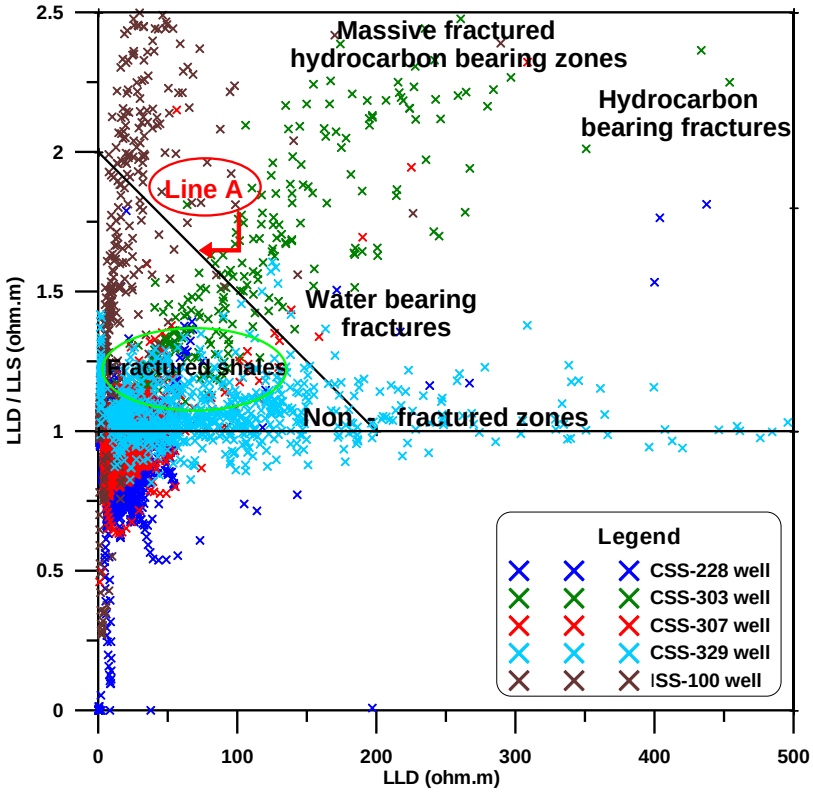

Figure 11: Crossplot of LLD/LLS versus LLD differentiated between fractured and unfractured zones in the lower dolomite rock unit.

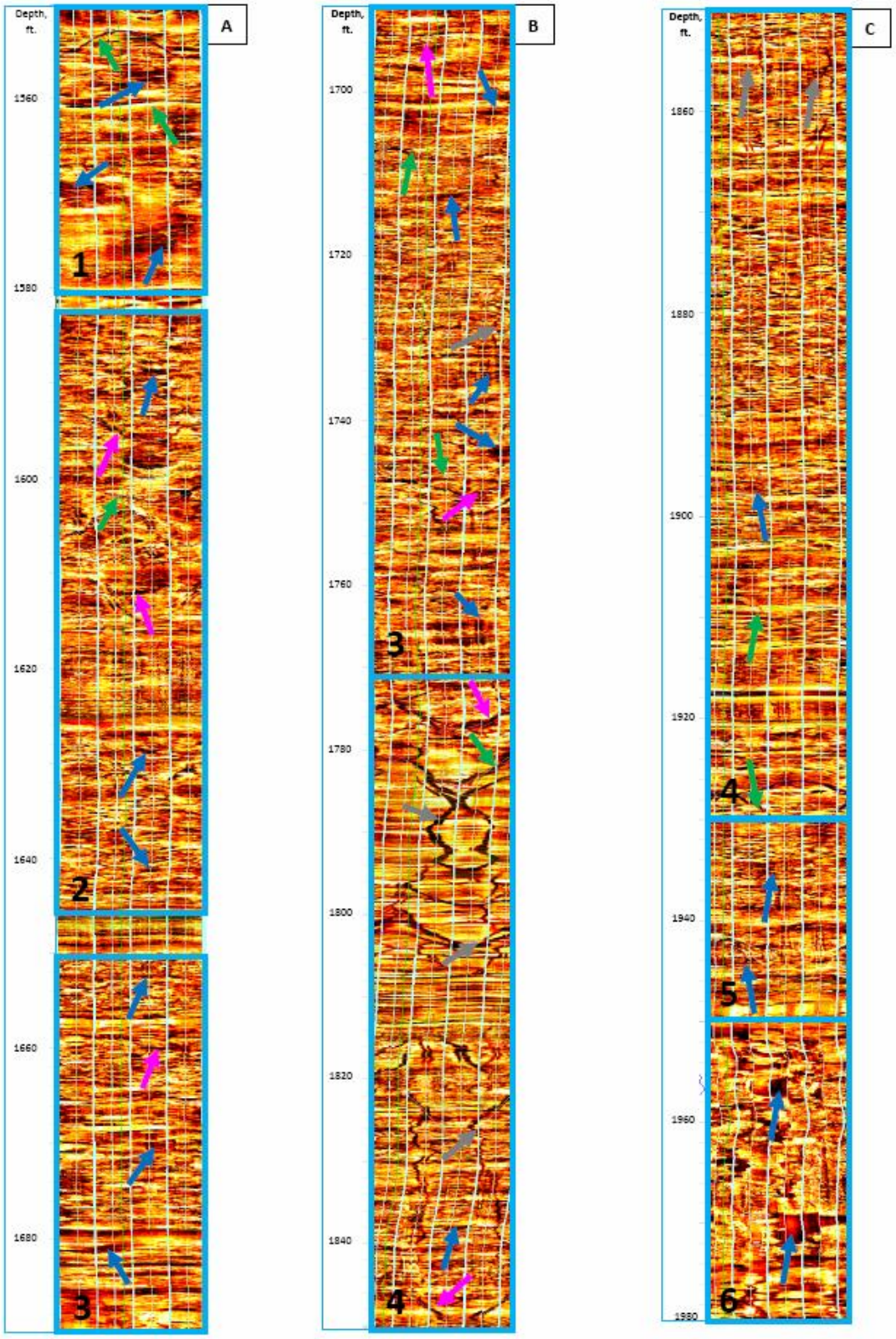

Figure 12: Formation Micro Imager (FMI) log showing secondary porosity structures detected in CSS-329 well: **(A);** 1550-1690 ft. **(B);** 1690-1850 ft. and **(C);** 1850-1980 ft. **1:** Large isolated vugs at 1550-1580 ft. and at 1950-1980 ft., **2:** Large interconnected vugs network at 1583-1646 ft., **3:** Interconnected vugs of various size 1650-1770 ft., **4:** Drilling-induced fractures interconnected to natural fractures (indicated by gray and green arrows) at 1770-1930 ft., **5:** Small interconnected vugs at 1930-1950 ft. and **6:** Dissolution channel (indicated by pink arrows).

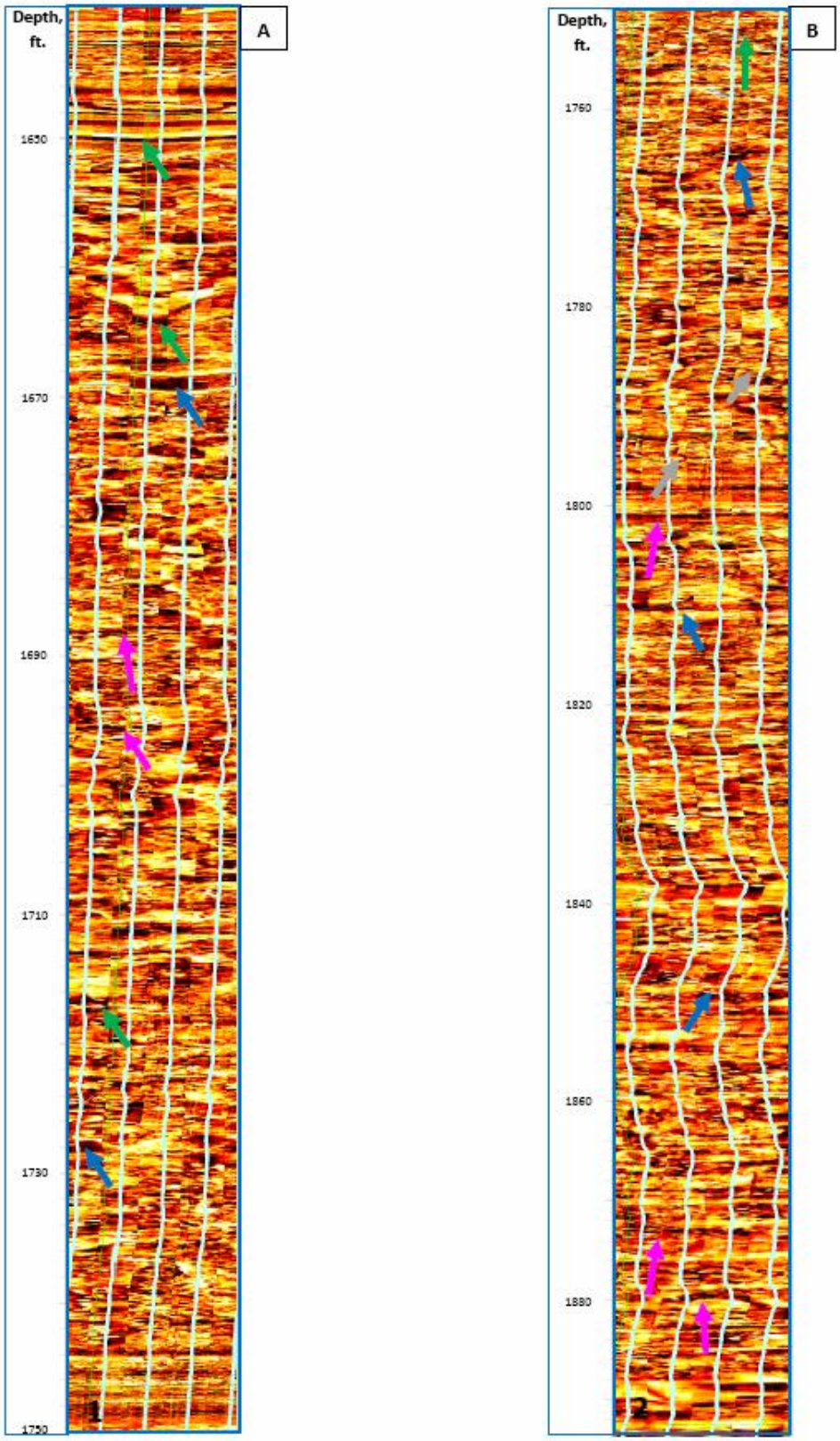

Figure 13: Formation Micro Imager (FMI) log showing secondary porosity structures detected in CSS-303 well: **(A);** 1640-1750 ft. and **(B);** 1751-1890 ft. **1:** Large highly interconnected vugs pores network at 1640-1750 ft. and **2:** Poorly interconnected vugs pores, drilling-induced fractures (indicated by gray and green arrows) and dissolution channel (indicated by pink arrows) at 1751-1890 ft.